Nontrivial topological electronic structures in a single Bi(111) bilayer on different substrates: A first-principles study

Zhi-Quan Huang,[1] Feng-Chuan Chuang,[1,*] Chia-Hsiu Hsu,[1] Yu-Tzu Liu,[1] Hua-Rong Chang,[1] Hsin Lin,[2,†] and Arun Bansil[2]

[1]*Department of Physics, National Sun Yat-Sen University, Kaohsiung 804, Taiwan*

[2]*Department of Physics, Northeastern University, Boston, Massachusetts 02115, USA*

(Received 30 May 2013; revised manuscript received 12 September 2013; published 1 October 2013)

Electronic structures, minimum energy configurations, and band topology of strained Bi(111) single bilayers placed on a variety of semiconducting and insulating substrates are investigated using first-principles calculations. A topological phase diagram of a free-standing Bi bilayer is presented to help guide the selection of suitable substrates. The insulating hexagonal-BN is identified as the best candidate substrate material for supporting nontrivial topological insulating phase of Bi bilayer thin films. A planar hexagonal Bi layer is predicted under tensile strain, which we show could be realized on a SiC substrate. The Bi bilayer becomes metallic under the compressive strain induced by Si and Ge substrates.

DOI: 10.1103/PhysRevB.88.165301 PACS number(s): 71.20.Nr, 73.20.At

The recent discovery of topological insulators (TIs) which possess a nontrivial Z_2 topological invariant is attracting worldwide attention, making this a fast developing area in materials sciences.[1–4] TIs host spin-polarized surface/edge states, which are not allowed to backscatter due to the constraint of time-reversal symmetry and are thus very desirable for spintronics and other applications.[5,6] The development of topological band theory combined with the predictive power of first-principles calculations, has led to the discovery of many new families of TIs such as Bi_2Se_3 (Refs. 7–11), $TlBiSe_2$ (Refs. 12 and 13), $GeBi_2Te_4$ (Ref. 14), half-Heuslers,[15–17] Li_2AgSb,[18] ternary tetradymite,[19] quaternary chalcogenides, and famatinites.[20] While a number of three-dimensional (3D) topological insulators have been realized experimentally, there are only very few materials realizations of the two-dimensional (2D) TIs, also referred to as quantum spin Hall (QSH) insulators. The key feature of a QSH insulator is the presence of protected gapless edge states which carry two spin-polarized currents propagating in opposite directions. Graphene was the first system which was proposed to support a QSH state through spin-orbit coupling effects, but the associated gap in graphene is too small to be accessible experimentally.[4] To date, the only experimental realizations of the QSH state are HgTe/CdTe (Refs. 21–23) and InAs/GaSb/AlSb (Refs. 24 and 25) quantum well systems. No stand-alone thin film or a thin film supported on a suitable substrate has been experimentally demonstrated to harbor a QSH state. The great need for finding new QSH insulator materials is for these reasons clear.

Theoretical studies have shown the sensitivity of the Z_2 topological invariant to film thickness in Bi_2Se_3 and Bi_2Te_3 ultrathin films,[26,27] suggesting that the 2D QSH phase could be induced through the reduced dimensionality in thin films of 3D TIs.[28–30] Accordingly, the search for 2D QSH phases has focused on Bi and Sb films in view of their strong spin-orbit interaction,[31–35] and the fact that Bi/Sb alloys were the first 3D TIs to be discovered experimentally.[36] In particular, a single Bi(111) bilayer (BL) film has been predicted to be an elemental 2D QSH insulator,[31,32] and ultrathin Bi(111) films are predicted to be topologically nontrivial for a wide range of film thicknesses.[33] In contrast, Sb(111) films with less than four Sb BLs are predicted to be topologically trivial,[35] but could become topologically non-trivial under tensile strain.[37] However, for practical applications, a thin film must be placed or grown on a substrate, which would influence both the crystal and the electronic structure of the film. But effects of the substrate on QSH candidate thin films are poorly understood, and to our knowledge, our study is the first to directly address the electronic structure of a supported Bi (111) bilayer for a wide variety of substrates. Our finding that out of the various substrates we examined, only *h*-BN would support the QHS state of a Bi (111) bilayer, reveals the key role of the substrate and gives insight into why it has been difficult to experimentally realize the Bi bilayer in the QSH state.

So motivated, we have investigated the electronic structure of a Bi(111) bilayer for a range of strains over a variety of semiconducting and insulating substrates using first-principles calculations. To guide the search for the most suitable substrates, we first study the effects of strain on free-standing thin films. Our analysis indicates that a Bi(111) single bilayer in the buckled honeycomb structure possesses a nontrivial band topology with topological invariant $Z_2 = 1$ over the entire range of strains examined here (<20%). While a nontrivial topological metal phase is predicted to occur under a compressive strain, the QSH insulating phase is found to exist not only at the relaxed lattice constant but also over a wide range of strains. Interestingly, we find that at a critical value of tensile strain the buckled honeycomb bilayer structure transforms into a more stable planar honeycomb structure. This structural change is found to induce a topological phase transition in which the buckling distance plays the key role.

The semiconducting and insulating substrates, which we have investigated, are Si(111)-1×1 (3.87 Å) (Ref. 38); Ge(111)-1×1 (4.09 Å); hexagonal-BN-$\sqrt{3}\times\sqrt{3}$ (4.53 Å); hexagonal-BN-2×2 (5.23 Å); and SiC(0001)-$\sqrt{3}\times\sqrt{3}$ (5.35 Å). These substrates encompass a fairly wide range to support various phases of a Bi(111) bilayer in buckled and planar structures. Our calculations show that the strong interaction with a Si or Ge substrate will destroy the insulating phase of the Bi bilayer. We identify hexagonal-BN as the best candidate substrate material to support the QSH insulating phase of Bi thin films. Moreover, we find large spin-split

states at Bi planar honeycomb structure on SiC(0001), which could be relevant for spintronics applications.

Calculations were carried out within the generalized gradient approximation (GGA) to the density-functional theory (DFT)[39–41] using the projector-augmented-wave (PAW) method[42] as implemented in the Vienna Ab Initio Simulation Package (VASP).[43] The kinetic energy cutoff was set to 400 eV and atomic positions were relaxed until the residual forces were less than 10^{-3} eV/Å. Spin-orbit coupling (SOC) was included in the band structure calculations. To model the single bilayer, a vacuum of ∼20 Å was included in the supercell. For bulk calculations, the Brillouin zone was sampled on a regular $21 \times 21 \times 21$ Monkhorst-Pack grid,[44] while a $21 \times 21 \times 1$ Monkhorst-Pack grid was used to sample the 2D Brillouin zone. Dispersive van der Waals (vdW) forces for the h-BN substrate were treated using the parameter setting optPBE-vdW which is described in detail in Ref. 45.

Free-standing thin films. The single Bi(111) bilayer structure is a buckled honeycomb structure, so that the bulk crystal of Bi, which is rhombohedral with two atoms per primitive cell, can be described as a stacking of these bilayers along the [111] direction. Assuming a hexagonal lattice, the lattice constants of bulk Bi obtained by optimizing the total energy are $a_0 = 4.58$ Å and $c_0 = 12.17$ Å, which agree well with previous studies.[46] The corresponding optimized equilibrium lattice constant a of a Bi single bilayer is 4.33 Å, which is 5.39% shorter than the aforementioned equilibrium bulk lattice constant, and the vertical distance between the two layers is found to be $d_1 = 1.74$ Å.

The total energy as a function of strain, defined with respect to the bulk lattice constant a_0, is shown in Fig. 1(a), where strain is modeled by varying the lateral lattice constant a_1 of the hexagonal lattice. The solid line (black dots) shows the results obtained when the bilayer structure is gradually subjected to an applied strain and atoms are allowed to relax. Also shown are the corresponding results (red dots) when the structure is constrained to remain flat, i.e., not allowed to buckle. We see that the honeycomb structure is energetically more favorable after $a_1 > 5.2$ Å. The black line in Fig. 1(a) shows that the buckled bilayer structure will transform into the more energetically favorable planar honeycomb structure ($d_1 = 0$) at around $a_1 = 5.5$ Å, provided the strain is applied gradually. The optimized lattice constant of the metastable planar honeycomb structure is found to be 5.27 Å.

Figure 1(b) shows how the band gap (black curve) of the buckled Bi bilayer evolves with strain. The gap is positive for $a_1 > 4.06$ Å so that the material is insulating, but it becomes metallic for $a_1 \leqslant 4.06$ Å as the gap values turn negative. The buckled bilayer remains insulating for $a_1 > 4.06$ Å until it transforms into the energetically favorable planar honeycomb structure, except that at 4.62 Å it is a zero-gap semiconductor as the conduction and valence bands touch each other at the Fermi level with parabolic dispersions and the band gap vanishes.

To delineate band topology, we identify the number of band inversions in the band structure, which can be inferred from the location of the s-type orbital at the high symmetry points in the Brillouin zone. [Note that the size of the black circles in Figs. 1(c) to 1(f) is proportional to the contribution of the s-type orbital.] Three states, labeled S_1, S_2, and S_3 at the

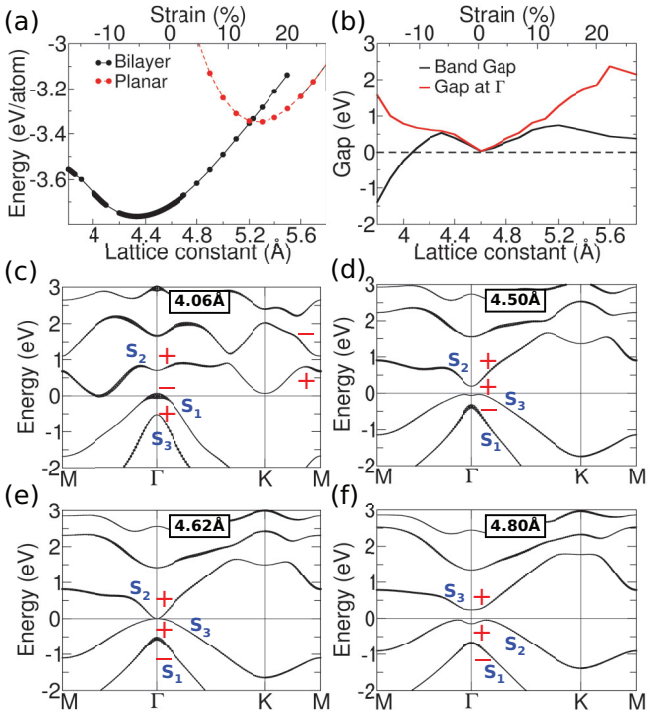

FIG. 1. (Color online) (a) Total energy of a free-standing Bi single bilayer in the buckled and planar honeycomb structures as a function of lattice constant. Corresponding strain values with respect to the lattice constant of crystalline Bi are marked on the top axis. (b) Band gap at the Γ point and the minimum band gap in the electronic spectrum as a function of lattice constant. (c)–(f) Band structures of free-standing Bi single bilayers in the buckled honeycomb lattice for various values of the lattice constant as marked in the figures. Size of the black circles is proportional to the contribution of the s-type orbital. The even and odd parities of the states are indicated by + and − signs, respectively.

Γ point are relevant. Among these, S_1 possesses the largest s-type character. We consider first Fig. 1(c) for the strain of −11.35% ($a_1 = 4.06$ Å) where the Bi(111) bilayer is seen to be a zero-gap semiconductor. Here, in the nonrelativistic band structure (not shown for brevity), S_1 lies at a higher energy than the degenerate states S_2 and S_3, i.e., $E_{S_1} > E_{S_2} = E_{S_3}$. The strong SOC in the Bi bilayer lifts the degeneracy between S_2 and S_3, and inverts the energy positions of S_1 and S_2, so that $E_{S_2} > E_{S_1}$ as shown in Fig. 1(c). This SOC induced band inversion between the conduction and valence bands at the Γ point is the hallmark of a nontrivial band topology. With increasing strain, S_1 gradually shifts downward in energy [see Fig. 1(d)]. At $a_1 = 4.37$ Å, valence levels S_1 and S_3 meet at Γ. As the strain increases further, conduction level S_2 meets valence level S_3 at a strain of $a_1 = 4.62$ Å, see Fig. 1(e). For $a_1 > 4.62$ Å, no band inversion is encountered, and the band structure remains topologically similar to that of Fig. 1(f) all the way up to $a_1 = 5.5$ Å, provided that the structure remains buckled.

To evaluate the topological invariant Z_2, we exploit the wave-function parity analysis.[47] For the Bi bilayer with zero strain, $a_1 = 4.58$ Å, parity eigenvalues below the Fermi level at the Γ and M points are in the order $+ - +$ and $+ - -$, respectively, from low to high energy. The corresponding products of the parity eigenvalues of the occupied valence

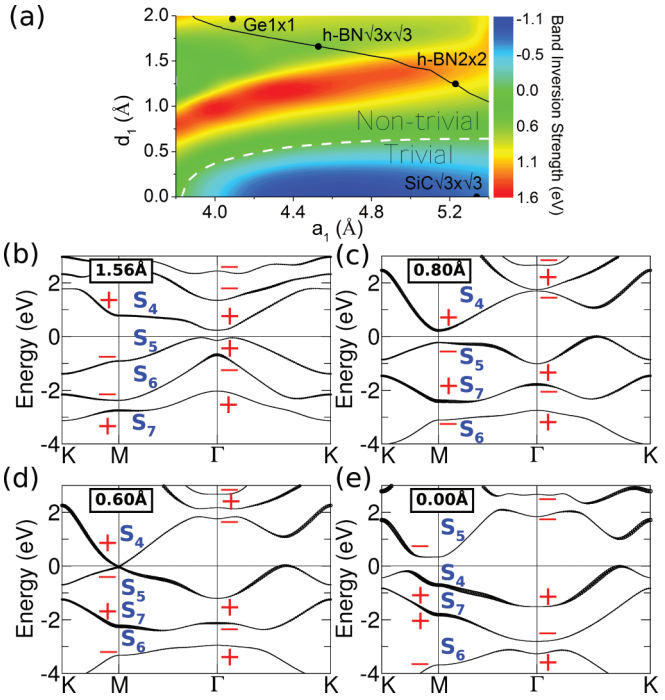

FIG. 2. (Color online) (a) The topological phase diagram for a free-standing Bi single bilayer thin film obtained from the band inversion strength E_I as a function of a_1 and d_1. The white dashed line separates the trivial and nontrivial topological phases. Values of d_1 (black line) as a function of lattice constant have been obtained by relaxing atomic positions of a free-standing Bi bilayer. The values of a_1 and d_1 for a Bi single bilayer for several representative substrates are identified. (b)–(e) Band structure evolution of the Bi bilayer as a function of the interlayer distance d_1 as shown in the figures. The buckled Bi bilayer transforms into the planar structure as d_1 goes to zero. The lateral lattice constant a_1 is kept fixed at 4.80 Å.

levels at Γ and M are -1 and 1, yielding the value $Z_2 = 1$ for the topological invariant.[32,48] As a_1 decreases to 4.37 Å, a band inversion between the S_1 level with odd parity and the S_3 level with even parity takes place at Γ [See Figs. 1(c) and 1(d)]. However, this does not change the topological invariant Z_2 since both states are below the Fermi level. In contrast, as a_1 increases to 4.62 Å, conduction level S_2 and the valence level S_3 meet each other at the Fermi level [Fig. 1(e)]. Since the gap closing at $a_1 = 4.62$ Å involves two states with the same parity, it is not a topological phase transition, but only realizes a zero-gap topological semimetal. The band topology of the Bi bilayers with tensile strains $a_1 > 4.62$ Å is also identified as being topological insulators with $Z_2 = 1$ as seen from Fig. 1(f). In short, our parity analysis indicates that the Bi bilayer is in a nontrivial topological state over the entire range of strains considered here where the system remains buckled. For $a_1 < 4.06$ Å, it is a topological metal, whereas for $a_1 > 4.06$ Å, it is a topological insulator, except at $a_1 = 4.62$ Å, where the Bi bilayer is a zero-gap topological semimetal.

As the buckled bilayer transforms into the planar honeycomb structure, the parity eigenvalues are in the order $+ - +$ (from low to high energy) at the Γ and $- + +$ at the M point [see Fig. 2(e)]. The product of the parity eigenvalues at either of these symmetry points is -1, yielding a trivial topological invariant $Z_2 = 0$, indicating that the planar honeycomb Bi layer is a topologically trivial insulator. This result also suggests that the buckling distance between the two layers in a Bi bilayer, d_1, is an important parameter for controlling band topology. Accordingly, in Figs. 2(b) to 2(e), we illustrate the band structure as a function of d_1 at $a_1 = 4.80$ Å, which can be regarded as a vertical path at $a_1 = 4.80$ Å in Fig. 2(a). Since no gap closing occurs at the Γ point over the entire range of d_1 values considered here, we need only to focus on the levels S_4–S_7 at the M point. The band topology in Figs. 2(b) and 2(c) is the same since no gap closing occurs between the conduction and valence bands as d_1 decreases from 1.56 to 0.80 Å even though S_6 and S_7 levels change their energy positions. As the distance d_1 is further reduced to 0.60 Å, the conduction level S_4 with even parity and valence level S_5 with odd parity meet at the M point, forming a linear Dirac-cone-like dispersion as shown in Fig. 2(d). This band inversion changes the product of parity for occupied states at the M point, resulting in a topological phase transition.

With the preceding understanding of how the band structure evolves with strain and buckling, we are in a position to introduce the quantity band-inversion strength (BIS) E_I, which provides a measure of how far the Bi bilayer system is from a topological critical point for any specific level of strain and/or buckling. From Fig. 2, the topological phase transition at the M point is driven by the band inversion between the S_4 and S_5 levels. Therefore, the energy difference between these two levels can be used as the BIS parameter for the M point as, $E_I^M = E_{S_4} - E_{S_5}$. The band inversion occurs when $E_I^M > 0$. As discussed already, the band inversion at the Γ point involves three levels S_1–S_3. The BIS at Γ for this reason is chosen to be the energy difference between the lowest conduction state with even parity and the S_1 level. From Fig. 1, when S_1 is occupied, either S_2 or S_3 is unoccupied. Thus, BIS at Γ can be expressed as $E_I^\Gamma = \max\{E_{S_2}, E_{S_3}\} - E_{S_1}$. Nontrivial band topology in the Bi bilayer thin film will occur when both E_I^M and E_I^Γ are positive. Therefore, the BIS of the system as a whole may be defined as, $E_I = \min\{E_I^M, E_I^\Gamma\}$. This quantity is positive only when the band topology of the system as a whole is nontrivial. This BIS parameter is a very useful measure of the robustness of a nontrivial topological phase. If E_I is small, one can expect that the band inversion required for nontrivial phase can be removed easily by perturbations. Figure 2(a) gives the BIS parameter E_I for Bi bilayer thin films as a function of a_1 and d_1. We will use this topological phase diagram to guide our search for suitable substrates by keeping in mind that a nontrivial phase will be more robust against perturbed environments by selecting substrates with lattice constant around 5 Å for which E_I is relatively large.

Effects of substrate. To utilize nontrivial topological properties of the Bi bilayer in the buckled or honeycomb structure, the Bi bilayer will need to be grown on an appropriate substrate. Accordingly, we have investigated the following semiconducting/insulating substrates: Si(111)-1×1 (3.87 Å); Ge(111)-1×1 (4.09 Å); h-BN-$\sqrt{3} \times \sqrt{3}$ (4.53 Å); h-BN-2×2 (5.23 Å); and SiC(0001)-$\sqrt{3} \times \sqrt{3}$ (5.35 Å). Substrates such as Si(111), Ge(111), and SiC(0001) can be expected to provide a significant perturbation to the deposited Bi bilayer. On the other hand, a weakly interacting substrate, e.g., h-BN, could

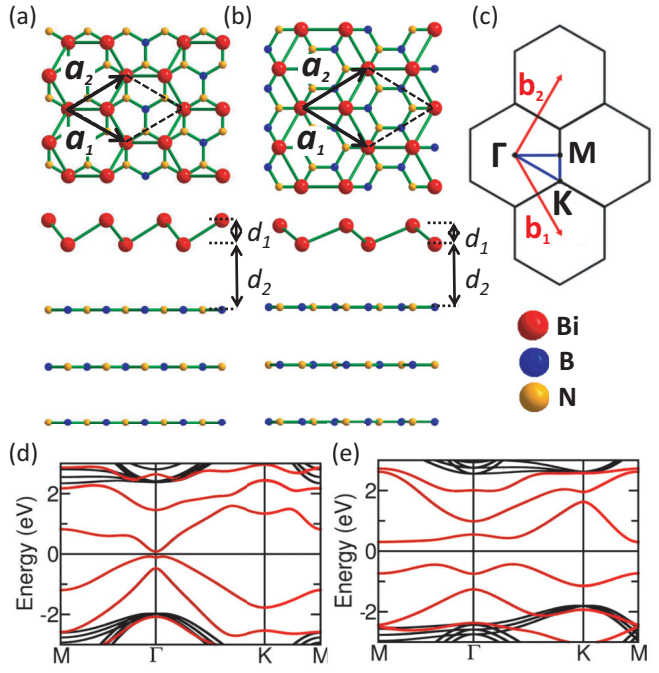

FIG. 3. (Color online) Atomic structure of the Bi bilayer on (a) h-BN $\sqrt{3}\times\sqrt{3}$ and (b) h-BN 2×2 substrate. (c) Surface Brillouin zone with high symmetry points marked. Surface band structure of the Bi bilayer on (d) h-BN $\sqrt{3}\times\sqrt{3}$ and (e) h-BN 2×2 substrate. Red bands are Bi-derived, while the black bands are derived from the substrate.

provide an excellent support to create a nearly free-standing 2D QSH system. All the candidate substrates presented in this article are worthy of further experimental study.[49] Notably, the presence of the substrate on one side of the thin film will break the inversion symmetry as is the case for a free-standing thin film in the presence of an external out-of-the-plane electric field.[50–52]

We consider the h-BN-$\sqrt{3}\times\sqrt{3}$ (4.53 Å) and h-BN-2×2 (5.23 Å) substrates first. The substrate is modeled by placing three BN layers under the Bi bilayer where atoms in the bottom BN layer are fixed at bulk crystalline positions. For the structural relaxation, van der Waals (vdW) forces[45] were included in the calculations. The coverage is 2/3 ML and 1/2 ML for h-BN-$\sqrt{3}\times\sqrt{3}$ and 2×2 structures, respectively, where one monolayer is defined as one Bi atom per B atom. We have examined energetics for numerous relative positions of the Bi bilayer relative to the h-BN where the lower layer of Bi atoms are on hollow site (above the center of beneath the BN hexagon), on top of B or N, or on top of B–N bond. We found these structures to be essentially degenerate in energy so long as the buckled structure is retained, with energy differences of less than 10 meV per supercell without vdW energies. Figures 3(a) and 3(b) show the lowest energy structures obtained by examining various different positions of the Bi bilayer relative to the substrate. The vertical distance d, is 3.697 or 3.578 Å for $\sqrt{3}\times\sqrt{3}$ or 2×2, respectively. For $\sqrt{3}\times\sqrt{3}$, all the Bi atoms lie on top of the N atoms. For 2×2, Bi atoms of the lower layer in the Bi bilayer lie on top of the B atoms, while the Bi atoms of the higher Bi layer lie on top of the N atoms. At $a_1 = 5.23$ Å the free-standing planar and buckled structures are nearly degenerate in energy, and these structures on the h-BN substrate are also found to be degenerate within tens of meV per supercell (without including the vdW contribution to energy). But, when the vdW energies are included, the free-standing buckled structure with as well as without the h-BN 2×2 substrate has a lower energy than the planar case. At coverage of 1/2 ML on h-BN 2×2, planar and buckled structures may coexist on the surface, and this coverage is not the best for supporting the nontrivial phase. On the other hand, $\sqrt{3}\times\sqrt{3}$ ($a_1 = 4.53$ Å) is close to the bulk lattice constant $a_0 = 4.58$ Å, so that this coverage will be the more viable one for supporting the topological insulator phase. The surface band structures of the Bi bilayer in the presence of the h-BN substrates, shown in Figs. 3(d) and 3(e), indicate that the Bi bilayer on h-BN essentially retains its electronic structure, and that the B and N atoms do not bond strongly with the Bi atoms.

To understand the stability of the Bi bilayer on h-BN, we define the formation energy, $E_f = \frac{1}{A}(E_{\rm tot} - E_{\rm sub} - N \times \mu_{Bi})$, where $E_{\rm tot}$ is the total energy of Bi bilayer on the h-BN surface, $E_{\rm sub}$ is the energy of the clean unreconstructed h-BN surface, A is the surface area of the supercell, $N = 2$ is the number of Bi atoms in the supercell, and $\mu_{\rm Bi}$ is the chemical potential of Bi. Calculating $E_{\rm tot}$ and $E_{\rm sub}$ by excluding van der Waals (vdW) energies, when $\mu_{\rm Bi}$ is set equal to the bulk energy of Bi, $E_{\rm bulk}$, the formation energy of the Bi bilayer on $\sqrt{3}\times\sqrt{3}$ h-BN is found to be lower than that on 2×2 h-BN by 15.6 meV/Å^2. At $(\mu_{\rm Bi} - E_{\rm bulk}) > -0.55$ eV, Bi bilayer on $\sqrt{3}\times\sqrt{3}$ h-BN (Bi coverage of 2/3 ML) is favored energetically.

Turning to larger strains or lattice constants where the Bi bilayer assumes the planar honeycomb structure, the candidate substrate for support is SiC(0001)-$\sqrt{3}\times\sqrt{3}$ (5.35 Å). The band structure of the free-standing Bi honeycomb at $a_1 = 5.35$ Å is

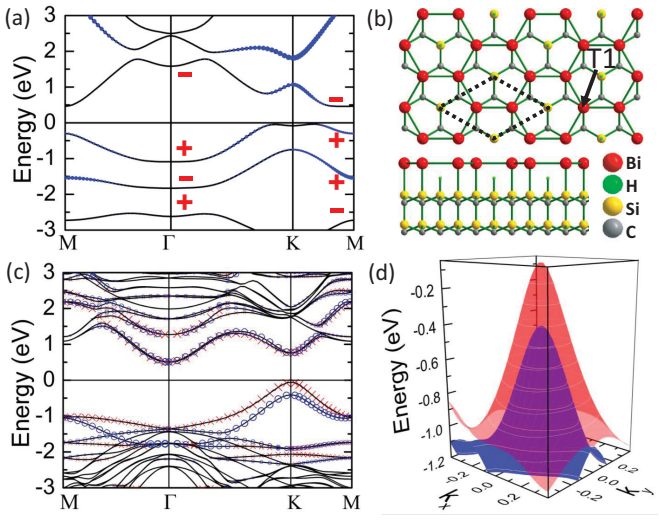

FIG. 4. (Color online) (a) Band structure of the free-standing Bi thin film in planar honeycomb structure at $a_1 = 5.35$ Å. (b) Atomic structure of Bi honeycomb on SiC(0001) $\sqrt{3}\times\sqrt{3}$ substrate. (c) Band structure of the Bi honeycomb on SiC(0001) $\sqrt{3}\times\sqrt{3}$. Red crosses and blue circles identify Bi-derived states with opposite spins. (d) Blow-up of the band structure of (c) around the K point. Red and blue colors refer to opposite spin-polarizations of the bands.

plotted in Fig. 4(a). Of the three possible positions of the Bi honeycomb on top of this substrate, the lowest energy is found for the case when the Bi atoms are on the $T1$ site. [Here we have adapted nomenclature from the Si(111) surface since SiC(0001) has a similar bilayer structure with the atop $T1$ site lying above the topmost Si atom.] Since there are three dangling bonds associated with Si atoms on the SiC(0001)-$\sqrt{3}\times\sqrt{3}$ surface, we used H atoms to passivate one of Si atoms in the cell. We show the resulting atomic model in Fig. 4(b), and the band structure of the Bi honeycomb on SiC(0001) in Fig. 4(c). In particular, the Bi planar honeycomb retains its trivial topological phase in the presence of this substrate. However, the substrate breaks the inversion symmetry of the Bi bilayer, and induces pronounced spin-splitting of bands around the K point, which is highlighted in the blow up of energy bands around the K point in Fig. 4(d). These spin-polarized states could be accessed by gating or hole-doping. Also, the large band gap as well as the large spin-splitting of valence states would make this Bi film attractive for room temperature applications.

The Bi bilayer transitions to the metallic phase for $a_1 <$ 4.06 Å. The relevant substrates here are Si(111) 1×1 and Ge(111) 1×1 with lattice constants of 3.87 and 4.09 Å, respectively. The lowest energy structures in this case, shown in Figs. 5(a) and 5(b), are found to be those in which the Bi atoms in the lower layer of the Bi bilayer lie on top of the centers of the hexagons. Band structures of the free-standing Bi bilayer at the lattice constants of the Si(111) and Ge(111) substrates are plotted in Figs. 5(c) and 5(d). The corresponding band structures when the Bi bilayer is placed on these substrates are shown in Figs. 5(e) and 5(f). The substrate is seen to induce substantial spin-splittings and charge transfers. The system will remain metallic even if the Fermi energy is shifted by doping/gating, so that in contrast to the h-BN substrate, the edge states in this case will overlap with bulk states. It will be interesting to investigate the extent to which the back-scattering transport channel becomes active under these conditions.[53]

Finally, we have investigated the effects of substrates on Sb bilayers along the preceding lines. This is interesting because Bi and Sb atoms belong to the same group of the periodic table, and both atoms exhibit large spin-orbit coupling. Strained free-standing Sb bilayers have been shown[37] to be a trivial semimetal for $a_1 <$ 3.84 Å, a trivial insulator for 3.84 Å $< a_1 <$ 4.49 Å, and a nontrivial insulator for $a_1 >$ 4.49 Å. We have carried out computations for Sb bilayers placed on various substrates considered in this study to obtain the associated minimum energy atomic structures and the related band structures, and generally find the effects of the substrates on Sb bilayers to be similar to those on Bi bilayers. For example, substantial spin-splittings are induced by Si(111) and Ge(111) substrates, and the Sb bilayer is found to be unstable on h-BN-2×2, transforming spontaneously into the planar honeycomb structure. Also, the Sb bilayer essentially retains its electronic structure when placed on h-BN-$\sqrt{3} \times \sqrt{3}$ or h-BN-2×2. However, a smaller spin-splitting of the valence band around the K point occurs for the Sb planar honeycomb on SiC(0001)-$\sqrt{3}\times\sqrt{3}$ compared to the Bi honeycomb on the same substrate.

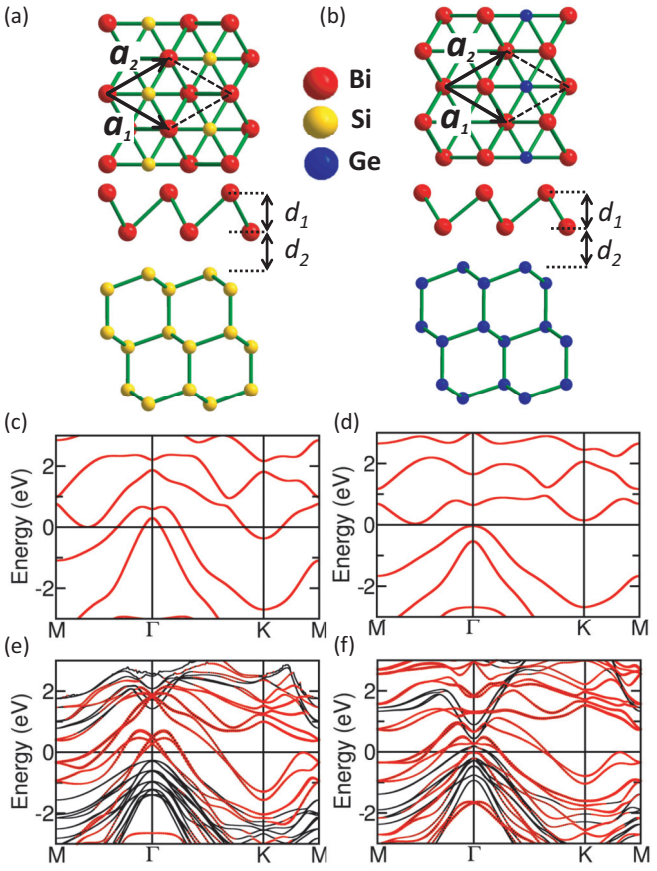

FIG. 5. (Color online) Atomic structure of Bi bilayer on (a) Si(111)-1×1 and (b) Ge(111))-1×1 substrate. Band structure of the free-standing Bi bilayer at the lattice constant of (c) 3.87 and (d) 4.09 Å. The band structure of Bi bilayer on (e) Si(111)-1×1 and (f) Ge(111))-1×1 surface. Red bands are Bi derived and the black bands are substrate derived.

To summarize, using first-principles computations, we have investigated the effects of a wide variety of insulating and semiconducting substrates on Bi bilayers over a wide range of strains. In this connection, the band topology of free-standing Bi bilayers is first delineated. The results are used to define a measure of band inversion strength, E_I, which provides us a basis for constructing a topological phase diagram of Bi bilayers for assessing the robustness of the nontrivial topological phases as a function of strain and/or the size of buckling. We identify the minimum energy configuration of the Bi bilayer for various substrates, and by examining the associated band structures, we delineate the characteristic effects of substrate on the geometry (buckled vs planar) and electronic properties (topologically interesting vs trivial insulator or metal) of the Bi bilayer. Our analysis indicates that insulating hexagonal-BN is the best candidate substrate material for supporting the nontrivial topological insulating phase of the Bi bilayer film. The SiC substrate, on the other hand, induces large spin and energy splittings, making this substrate interesting for spintronics applications. Our study gives insight into why it has been difficult to realize a Bi bilayer experimentally, and it will spur targeted efforts using an h-BN substrate to realize the QSH state in a Bi bilayer, which is of great current interest.

F.C.C. acknowledges support from the National Center for Theoretical Sciences and the Taiwan National Science Council under Grant No. NSC-101-2112-M110-002-MY3, and is grateful to the National Center for High-Performance Computing for computer time and facilities. The work at Northeastern University is supported by the U.S. Department of Energy, Office of Science, Basic Energy Sciences Contract No. DE-FG02-07ER46352, and benefited from theory support at the Advanced Light Source and the allocation of supercomputer time at NERSC through DOE Grant No. DE-AC02-05CH11231.

*fchuang@mail.nsysu.edu.tw
†nilnish@gmail.com

[1] J. E. Moore, Nature (London) **464**, 194 (2010).
[2] M. Z. Hasan and C. L. Kane, Rev. Mod. Phys. **82**, 3045 (2010).
[3] X.-L. Qi and S.-C. Zhang, Rev. Mod. Phys. **83**, 1057 (2011).
[4] C. L. Kane and E. J. Mele, Phys. Rev. Lett. **95**, 146802 (2005).
[5] B. A. Bernevig and S.-C. Zhang, Phys. Rev. Lett. **96**, 106802 (2006).
[6] C. Xu and J. E. Moore, Phys. Rev. B **73**, 045322 (2006).
[7] Y. S. Hor, A. Richardella, P. Roushan, Y. Xia, J. G. Checkelsky, A. Yazdani, M. Z. Hasan, N. P. Ong, and R. J. Cava, Phys. Rev. B **79**, 195208 (2009).
[8] D. Hsieh, Y. Xia, D. Qian, L. Wray, J. H. Dil, F. Meier, J. Osterwalder, L. Patthey, J. G. Checkelsky, N. P. Ong, A. V. Fedorov, H. Lin, A. Bansil, D. Grauer, Y. S. Hor, R. J. Cava, and M. Z. Hasan, Nature (London) **460**, 1101 (2009).
[9] S. R. Park, W. S. Jung, C. Kim, D. J. Song, C. Kim, S. Kimura, K. D. Lee, and N. Hur, Phys. Rev. B **81**, 041405 (2010).
[10] Y. L. Chen, J. G. Analytis, J.-H. Chu, Z. K. Liu, S.-K. Mo, X. L. Qi, H. J. Zhang, D. H. Lu, X. Dai, Z. Fang, S. C. Zhang, I. R. Fisher, Z. Hussain, and Z.-X. Shen, Science **325**, 178 (2009).
[11] D. Hsieh, Y. Xia, D. Qian, L. Wray, F. Meier, J. H. Dil, J. Osterwalder, L. Patthey, A. V. Fedorov, H. Lin, A. Bansil, D. Grauer, Y. S. Hor, R. J. Cava, and M. Z. Hasan, Phys. Rev. Lett. **103**, 146401 (2009).
[12] H. Lin, R. S. Markiewicz, L. A. Wray, L. Fu, M. Z. Hasan, and A. Bansil, Phys. Rev. Lett. **105**, 036404 (2010).
[13] S.-Y. Xu, Y. Xia, L. A. Wray, S. Jia, F. Meier, J. H. Dil, J. Osterwalder, B. Slomski, A. Bansil, H. Lin, R. J. Cava, and M. Z. Hasan, Science **332**, 560 (2011).
[14] M. Neupane, S.-Y. Xu, L. A. Wray, A. Petersen, R. Shankar, N. Alidoust, C. Liu, A. Fedorov, H. Ji, J. M. Allred, Y. S. Hor, T.-R. Chang, H.-T. Jeng, H. Lin, A. Bansil, R. J. Cava, and M. Z. Hasan, Phys. Rev. B **85**, 235406 (2012).
[15] H. Lin, L. A. Wray, Y. Xia, S. Xu, S. Jia, R. J. Cava, A. Bansil, and M. Z. Hasan, Nat. Mater. **9**, 546 (2010).
[16] S. Chadov, X. Qi, J. Kübler, G. H. Fecher, C. Felser, and S. C. Zhang, Nat. Mater. **9**, 541 (2010).
[17] W. Al-Sawai, H. Lin, R. S. Markiewicz, L. A. Wray, Y. Xia, S.-Y. Xu, M. Z. Hasan, and A. Bansil, Phys. Rev. B **82**, 125208 (2010).
[18] H. Lin, T. Das, Y. J. Wang, L. A. Wray, S.-Y. Xu, M. Z. Hasan, and A. Bansil, Phys. Rev. B **87**, 121202 (2013).
[19] H. Lin, T. Das, L. A. Wray, S.-Y. Xu, M. Z. Hasan, and A. Bansil, New J. Phys. **13**, 095005 (2011).
[20] Y. J. Wang, H. Lin, T. Das, M. Z. Hasan, and A. Bansil, New J. Phys. **13**, 085017 (2011).
[21] B. A. Bernevig, T. L. Hughes, and S.-C. Zhang, Science **314**, 1757 (2006).
[22] M. König, S. Wiedmann, C. Brüne, A. Roth, H. Buhmann, L. W. Molenkamp, X.-L. Qi, and S.-C. Zhang, Science **318**, 766 (2007).
[23] A. Roth, C. Brüne, H. Buhmann, L. W. Molenkamp, J. Maciejko, X.-L. Qi, and S.-C. Zhang, Science **325**, 294 (2009).
[24] C. Liu, T. L. Hughes, X.-L. Qi, K. Wang, and S.-C. Zhang, Phys. Rev. Lett. **100**, 236601 (2008).
[25] I. Knez, R.-R. Du, and G. Sullivan, Phys. Rev. Lett. **107**, 136603 (2011).
[26] H.-Z. Lu, W.-Y. Shan, W. Yao, Q. Niu, and S.-Q. Shen, Phys. Rev. B **81**, 115407 (2010).
[27] C.-X. Liu, H. J. Zhang, B. Yan, X.-L. Qi, T. Frauenheim, X. Dai, Z. Fang, and S.-C. Zhang, Phys. Rev. B **81**, 041307 (2010).
[28] Notably, a Bi (111) bilayer has been realized experimentally on Bi_2Te_3 (Refs. 29 and 30). But the surface of a topological insulator such as Bi_2Te_3 is guaranteed to support gapless metallic states. Therefore, it is not clear how a Bi bilayer on a topological insulator substrate will be able to realize an insulating state.
[29] Toru Hirahara, Gustav Bihlmayer, Yusuke Sakamoto, Manabu Yamada, Hidetoshi Miyazaki, Shin-ichi Kimura, Stefan Blugel, and Shuji Hasegawa, Phys. Rev. Lett. **107**, 166801 (2011).
[30] T. Hirahara, N. Fukui, T. Shirasawa, M. Yamada, M. Aitani, H. Miyazaki, M. Matsunami, S. Kimura, T. Takahashi, S. Hasegawa, and K. Kobayashi, Phys. Rev. Lett. **109**, 227401 (2012).
[31] S. Murakami, Phys. Rev. Lett. **97**, 236805 (2006).
[32] M. Wada, S. Murakami, F. Freimuth, and G. Bihlmayer, Phys. Rev. B **83**, 121310 (2011).
[33] Z. Liu, C.-X. Liu, Y.-S. Wu, W.-H. Duan, F. Liu, and J. Wu, Phys. Rev. Lett. **107**, 136805 (2011).
[34] G. Bian, T. Miller, and T.-C. Chiang, Phys. Rev. Lett. **107**, 036802 (2011).
[35] P. F. Zhang, Z. Liu, W. Duan, F. Liu, and J. Wu, Phys. Rev. B **85**, 201410 (2012).
[36] D. Hsieh, D. Qian, L. Wray, Y. Xia, Y. S. Hor, R. J. Cava, and M. Z. Hasan, Nature (London) **452**, 970 (2008).
[37] F.-C. Chuang, C.-H. Hsu, C.-Y. Chen, Z.-Q. Huang, V. Ozolins, H. Lin, and A. Bansil, Appl. Phys. Lett. **102**, 022424 (2013).
[38] C.-H. Hsu, W.-H. Lin, V. Ozolins, and F.-C. Chuang, Phys. Rev. B **85**, 155401 (2012).
[39] P. Hohenberg and W. Kohn, Phys. Rev. **136**, B864 (1964); W. Kohn and L. J. Sham, *ibid.* **140**, A1133 (1965).
[40] D. M. Ceperley and B. J. Alder, Phys. Rev. Lett. **45**, 566 (1980).
[41] J. P. Perdew and A. Zunger, Phys. Rev. B **23**, 5048 (1981).
[42] G. Kresse and D. Joubert, Phys. Rev. B **59**, 1758 (1999).
[43] G. Kresse and J. Hafner, Phys. Rev. B **47**, 558 (1993); G. Kresse and J. Furthmüller, *ibid.* **54**, 11169 (1996).
[44] H. J. Monkhorst and J. D. Pack, Phys. Rev. B **13**, 5188 (1976).
[45] J. Klimes, D. R. Bowler, and A. Michaelides, Phys. Rev. B **83**, 195131 (2011).
[46] X. Gonze, J.-P. Michenaud, and J.-P. Vigneron, Phys. Rev. B **41**, 11827 (1990).

[47] L. Fu and C. L. Kane, Phys. Rev. B **76**, 045302 (2007).

[48] Our results for the Bi bilayer without strain are the same as those reported by Wada *et al*. (Ref. 32).

[49] All the systems considered in this study are cases that a 1×1 unit cell of Bi bilayer are placed on the substrates with their lattice constants fall within $3.8\,\text{Å} < a_1 < 5.4\,\text{Å}$. No exhaustive search in other lowest energy structures for larger supercells or different coverages was performed.

[50] With regard to observing a Bi bilayer on *h*-BN via angle-resolved photoemission spectroscopy (ARPES) and scanning tunneling microscope (STM), we should keep in mind the well-known complications associated with wide band-gap substrates (Ref. 51), which require heavy doping to apply a bias voltage, and the difficulties of interpreting spectra due to effects of the ARPES/STM matrix element (Ref. 52).

[51] Jiamin Xue, Javier Sanchez-Yamagishi, Danny Bulmash, Philippe Jacquod, Aparna Deshpande, K. Watanabe, T. Taniguchi, Pablo Jarillo-Herrero, and Brian J. LeRoy, Nat. Mater. **10**, 282 (2011); Chia-Hsiu Hsu, Vidvuds Ozolins, and Feng-Chuan Chuang, Surf. Sci. **616**, 149 (2013); J. F. Zheng, X. Liu, N. Newman, E. R. Weber, D. F. Ogletree, and M. Salmeron, Phys. Rev. Lett. **72**, 1490 (1994).

[52] S. Sahrakorpi, M. Lindroos, R. S. Markiewicz, and A. Bansil, Phys. Rev. Lett. **95**, 157601 (2005); A. Bansil, M. Lindroos, S. Sahrakorpi, and R. S. Markiewicz, Phys. Rev. B **71**, 012503 (2005); Susmita Basak, Tanmoy Das, Hsin Lin, J. Nieminen, M. Lindroos, R. S. Markiewicz, and A. Bansil, *ibid*. **80**, 214520 (2009); J. Nieminen, H. Lin, R. S. Markiewicz, and A. Bansil, Phys. Rev. Lett. **102**, 037001 (2009).

[53] B.-J. Yang, M. S. Bahramy, and N. Nagaosa, Nat. Commun. **4**, 1524 (2013).